Available online at www.easdprocedia.org
EASD Procedia EURODYN (2020) 1178-1188

EASD Procedia

EURODYN 2020
XI International Conference on Structural Dynamics
M. Papadrakakis, M. Fragiadakis, C. Papadimitriou (eds.)
Athens, Greece, 23–26 November 2020

MONITORING FATIGUE DAMAGE ACCUMULATION OF WIND TURBINE TOWERS USING LIMITED NUMBER OF OUTPUT-ONLY VIBRATION MEASUREMENTS

Victor Flores Terrazas[1], Omid Sedehi[1], Lambros S. Katafygiotis[1], Costas Papadimitriou[2]

[1] The Hong Kong University of Science and Technology
Department of Civil and Environmental Engineering
Hong Kong, China
vft@connect.ust.hk, osedehi@connect.ust.hk, katafygiotis.lambros@gmail.com

[2]University of Thessaly
Department of Mechanical Engineering
Volos, Greece
costasp@uth.gr

Keywords: Multiaxial Loading, Fatigue Damage Accumulation, Wind Turbines, Bayesian Methods, Input-State Estimation

Abstract. *Fatigue monitoring and remaining fatigue life estimation of structures using output-only vibration measurements has recently garnered increasing attention, producing advances in theoretical, numerical and experimental studies of this phenomenon. The methodology presented in this paper combines methods for estimating stress time histories at the entire body of the structure with fatigue damage accumulation techniques for multiaxial stress state. A novel sequential Bayesian method is employed to estimate both input and state in the modal space and to reconstruct the full-field time-history response in the physical space using output-only vibration measurements. Stress and strain time histories at the finite element level are obtained by using a linear relationship with nodal displacements. Estimated stresses are then used to find the critical plane where the maximum fatigue damage is expected and the shear stress time histories are resolved on this plane. Shear stress cycles are counted by means of the Rainflow Counting Method, and a Modified Wöhler Curve Method is applied to estimate the fatigue damage, whereby normal and shear stress effects are accounted for. This procedure is capable of tackling inherent complexities found in real world applications, such as the multiaxiality of the applied loads and of the resulting stress state. A finite element model of a wind turbine tower was constructed based on reference specifications available from the National Renewable Energy Laboratory and used to illustrate the method presented herein. The results obtained demonstrate the applicability of the methodology as an efficient way to monitor fatigue damage accumulation in the entire body of a steel structure.*

ISSN:2311-9020 © 2020 The Authors. Published by EASD Procedia.
Peer-review under responsibility of the Organizing Committee of EURODYN 2020.
doi: 10.47964/1120.9094.19302

1 INTRODUCTION

Fatigue damage accumulation in ductile materials does not always produce identifiable indicators of damage. Thus, it is important to develop monitoring methods that would enable to diagnose the fatigue state of a metallic structure and to predict the location(s) where high fatigue damage is most likely to accumulate, as well as the remaining fatigue lifetime of the structure, based on output only vibration measurements.

The work by Papadimitriou et al. [1] was the first to promote the use of output-only vibration measurements to estimate fatigue damage accumulation. It introduced the idea of using a Kalman filter to estimate the stress responses of a metallic structure subjected to stationary stochastic loads, thereby estimating the remaining fatigue lifetime. Nevertheless, this approach and subsequent ones [2]–[4] developed to handle non-stationary unknown excitations, considered uniaxial fatigue damage. The present work expands on this idea and applies techniques capable of handling multiaxial stress states.

Thereupon model reduction techniques have been introduced and used in conjunction with SHM methods, e.g., modal decomposition-expansion was employed by Maes et al. [5] to reconstruct the dynamic strain response of an offshore wind turbine tower; Tchemodanova et al. demonstrated in [6] the use of a substructure approach to estimate remaining fatigue lifetime of a section of a rollercoaster; Eftekhar Azam et al. proposed the use of a Dual Kalman in modal space, allowing the use of a modally truncated model [7].

The purpose of this work is to propose a methodology to monitor fatigue damage accumulation on a structural system or its components when subjected to input or interface loads that are unknown. The present work expands on ideas presented in [3], [8] for response reconstruction and fatigue estimation in linear components of structural systems and applies techniques capable of handling multiaxial stress fields. Moreover, it benefits from the latest advances accomplished in the area of joint input-state estimation [7], [9]–[12], adopting a novel sequential Bayesian approach to reconstruct the full-field dynamic responses using sparse output-only measurements.

The organization of this work is as follows. In Section 2, we present pertinent mathematical formulations for the strain/stress response reconstruction of the entire structure by means of the novel sequential Bayesian filtering technique presented in Section 3. In Section 4, we outline the formulations for the full-field multiaxial fatigue damage accumulation. Section 5 shows an illustrative example of the application of the proposed methodology on a FE model of a land-based wind turbine tower structure subjected to wind loads. Lastly, conclusions are put forth in Section 6.

2 MATHEMATICAL FORMULATION FOR STRAIN/STRESS ESTIMATION

2.1 System and observation models

The dynamical response of a linear time-invariant system can be described through Newton's second law of motion:

$$\boldsymbol{M}\ddot{\boldsymbol{x}}(t) + \boldsymbol{C}\dot{\boldsymbol{x}}(t) + \boldsymbol{K}\boldsymbol{x}(t) = \boldsymbol{S}_p\boldsymbol{f}(t) \tag{1}$$

where $\boldsymbol{M} \in \mathbb{R}^{N\times N}, \boldsymbol{C} \in \mathbb{R}^{N\times N}, \boldsymbol{K} \in \mathbb{R}^{N\times N}$, are the mass, damping and stiffness matrices, respectively; N is the number of degrees-of-freedom; $\boldsymbol{f}(t) \in \mathbb{R}^{N_I\times 1}$, is the dynamic force vector comprised of N_I independent components; $\boldsymbol{S}_p(t) \in \mathbb{R}^{N_I\times 1}$ is a matrix characterizing the spatial distribution of external forces; $\ddot{\boldsymbol{x}}(t) \in \mathbb{R}^{N\times 1}$, $\dot{\boldsymbol{x}}(t) \in \mathbb{R}^{N\times 1}$ and $\boldsymbol{x}(t) \in \mathbb{R}^{N\times 1}$ are the acceleration, velocity, and displacement responses, respectively. When the vibration response is transformed into a truncated modal space, the following equation of motion is obtained [9]:

$$\ddot{\boldsymbol{\zeta}}(t) + \boldsymbol{\Gamma}\dot{\boldsymbol{\zeta}}(t) + \boldsymbol{\Omega}^2\boldsymbol{\zeta}(t) = \boldsymbol{\Phi}^T\boldsymbol{S}_p\boldsymbol{f}(t) \tag{2}$$

where $\boldsymbol{\Phi} \in \mathbb{R}^{N\times N_m}$ is the truncated modal matrix whose columns are filled with N_m mass-normalized mode shape vectors; $\boldsymbol{\zeta}(t) \in \mathbb{R}^{N_m\times 1}$ is the response in the reduced modal space; $\boldsymbol{\Gamma} \in \mathbb{R}^{N_m\times N_m}$ and $\boldsymbol{\Omega}^2 \in \mathbb{R}^{N_m\times N_m}$ are two diagonal matrices with $2\xi_i\omega_i$ and ω_i^2 entries, respectively; ξ_i and ω_i are, correspondingly, the modal damping ratio and modal frequency of the ith dynamical mode. This equation can be written in the state-space form as follows:

$$\dot{\boldsymbol{z}}(t) = \boldsymbol{A}_C\boldsymbol{z}(t) + \boldsymbol{B}_C\boldsymbol{f}(t) \tag{3}$$

where $\boldsymbol{z}(t) = \begin{bmatrix}\boldsymbol{\zeta}(t)^T & \dot{\boldsymbol{\zeta}}(t)^T\end{bmatrix}^T$ is the state vector; $\boldsymbol{A}_C$ and $\boldsymbol{B}_C$ are the system and feedthrough matrices, computed as:

$$\boldsymbol{A}_C = \begin{bmatrix}\boldsymbol{0} & \boldsymbol{I}\\ -\boldsymbol{\Omega}^2 & -\boldsymbol{\Gamma}\end{bmatrix}\ ,\ \boldsymbol{B}_C = \begin{bmatrix}\boldsymbol{0}\\ \boldsymbol{\Phi}^T\boldsymbol{S}_p\end{bmatrix} \tag{4}$$

When the responses are discretized in Δt intervals and the variation of input forces is considered to be constant over each interval, the following stochastic state-space model is obtained in the discrete-time:

$$\boldsymbol{z}_k = \boldsymbol{A}\boldsymbol{z}_{k-1} + \boldsymbol{B}\boldsymbol{f}_{k-1} + \boldsymbol{v}_k \tag{5}$$

where $\boldsymbol{A} = e^{\boldsymbol{A}_C\Delta t}$ and $\boldsymbol{B} = (\boldsymbol{A} - \boldsymbol{I})\boldsymbol{A}_C^{-1}\boldsymbol{B}_C$ are the discrete-time system and feedthrough matrices; $\boldsymbol{z}_k$ is the state vector at $t_k = k\Delta t\ ,\ k = \{0,1,2,\dots,n\}$; $\boldsymbol{v}_k$ is the process noise modeled as a Gaussian White Noise (GWN) process.

In a similar manner, the observed output quantities of interest can be written as a function of the state vector and the input forces leading to [7]:

$$\boldsymbol{d}_k \triangleq \begin{bmatrix}\boldsymbol{\varepsilon}_k\\ \boldsymbol{y}_k\\ \dot{\boldsymbol{y}}_k\\ \ddot{\boldsymbol{y}}_k\end{bmatrix} = \boldsymbol{G}\boldsymbol{z}_k + \boldsymbol{J}\boldsymbol{f}_k + \boldsymbol{w}_k \tag{6}$$

$$\boldsymbol{G} = \begin{bmatrix}\boldsymbol{S}_e\boldsymbol{T}\boldsymbol{\Phi} & \boldsymbol{0}\\ \boldsymbol{S}_d\boldsymbol{\Phi} & \boldsymbol{0}\\ \boldsymbol{0} & \boldsymbol{S}_v\boldsymbol{\Phi}\\ -\boldsymbol{S}_a\boldsymbol{\Phi}\boldsymbol{\Omega}^2 & -\boldsymbol{S}_a\boldsymbol{\Phi}\boldsymbol{\Gamma}\end{bmatrix}\ ,\ \boldsymbol{J} = \begin{bmatrix}\boldsymbol{0}\\ \boldsymbol{0}\\ \boldsymbol{0}\\ \boldsymbol{S}_a\boldsymbol{\Phi}\boldsymbol{\Phi}^T\boldsymbol{S}_p\end{bmatrix} \tag{7}$$

where $\boldsymbol{d}_k \in \mathbb{R}^{N_o\times 1}$ is a vector containing the observed quantities at discrete time t_k, comprised by strains $\boldsymbol{\varepsilon}_k \in \mathbb{R}^{N_e\times 1}$, displacements $\boldsymbol{y}_k \in \mathbb{R}^{N_y\times 1}$, velocities $\dot{\boldsymbol{y}}_k \in \mathbb{R}^{N_{\dot{y}}\times 1}$, and accelerations $\ddot{\boldsymbol{y}}_k \in \mathbb{R}^{N_{\ddot{y}}\times 1}$; the matrices $\boldsymbol{S}_d, \boldsymbol{S}_v, \boldsymbol{S}_a$ and $\boldsymbol{S}_e$ are selection matrices consisting of 0's and 1's used to extract the observed DOF; $\boldsymbol{T}$ is a matrix returning local strains from nodal displacements; $\boldsymbol{w}_k$ is observation noise considered to be GWN.

3 BAYESIAN ESTIMATION OF INPUT AND STATE

We build our method upon the foregoing state-space formulations and the sequential Bayesian method developed in [11], [13]. The reader is referred to [13] for detailed nomenclature and mathematical formulations. This implementation allows estimating the system state and input in real-time based on a limited number of output-only measurements. Another advantage of this novel algorithm is its robust capability to update the process and observation noise covariance matrices in an online manner. On the other hand, a caveat to this method is that, similar to other Kalman-type filters, some initial parameters need to be fine-tuned to achieve best results; for the sequential Bayesian filter, these parameters are the initial covariance matrices. A good starting point to calibrate the filter is to set the initial state and input covariance matrices equal to identity matrices scaled by a very small number. A more accurate, albeit laborious approach to selecting appropriate initial noise parameters, is to consider different orders of magnitude for the elements the initial estimates for the covariance matrices, in accordance to the modal response quantities (displacement, velocity, acceleration) to which the element corresponds [14].

4 FATIGUE ASSESSMENT

4.1 Maximum Variance Method for locating the critical plane

The so-called critical plane approaches are based on the assumption that fatigue life is mainly dependent on cracks developing along shear planes or tensile planes [15]. Thus, the maximum fatigue damage experienced in an element can be expected to occur at such orientation. To find such orientation, we adopt the use of the Maximum Variance Method (MVM) proposed by Susmel et al. [16]. This method assumes that the critical plane lies along the direction which is anticipated to have the maximum shear stress variation; the rationale stems from the definition of the statistical variance, which measures how much the signal deviates from the mean. Since fatigue damage is caused by cyclic loading, the variance can be an appropriate measure to identify the plane where the signal presents the largest variation range. Therefore, the damage is expected to be the greatest at the aforementioned plane. The advantage of this method lies in that, once the critical plane is found, the shear stress signals can be readily resolved along this orientation by a simple stress transformation.

Lastly, it should be noted that by applying the MVM, the critical plane and its corresponding shear stress are obtained. The latter is a unidimensional parameter, so a cycle counting method, such as the Rainflow Counting Method (RCM), can be used directly with the resolved shear stress signal.

4.2 Modified Wöhler Curve Method for fatigue assessment

In addition to the MVM described above, Susmel et al. [17] formulated the so-called Modified Wöhler Curve Method (MWCM) to be used as a companion method. The motivation behind this method is that the MVM and subsequent cycle counting is based on shear stresses resolved along the critical plane; however, this stress signal alone may fail to account for the multiaxiality of the actual stress state. As such, a modification in the SN-Curve is introduced to account for the level of multiaxiality by considering the stress normal to the critical plane. Ultimately, a modified fatigue lifetime curve is obtained.

For brevity, the detailed formulations of the MWCM are omitted in this paper. The reader is thus referred to [17], [18] for a comprehensive explanation of this method and an illustrative example.

4.3 Fatigue damage accumulation

The last step in the fatigue assessment framework is to use the data generated throughout and to calculate the accumulated damage in the whole structure. The damage accumulation model used herein is the linear Palmgren-Miner's rule, which states that the linear fatigue accumulation damage D is found by [19], [20]:

$$D = \sum_{i=1}^{j} \frac{n_i}{N_{f,i}} \tag{8}$$

where j is the number of different amplitude levels found through RCM; n_i is the number of counted cycles at a given amplitude level, and $N_{f,i}$ is the number of cycles to failure at amplitude level i, found directly in the constructed MWC.

Once the appropriate SN-Curve has been obtained from the MWCM, and the RCM has been applied to the time history of the shear stress relative to the critical plane, this information can then be used to compute the accumulated fatigue damage for each element in the finite element model of the structure. The procedure is repeated for every finite element in the discretized model. The final product is a full-field damage accumulation map.

5 NUMERICAL EXAMPLE

A reference land-based wind turbine tower model was used in this study. Physical and material specifications were obtained from the National Renewable Energy Laboratory (NREL) [21], from which a finite element model (FEM) was constructed. For simplicity, the dynamic response of the rotor nacelle assembly (RNA) was modelled by an equivalent system of forces at the RNA-tower interface, as shown schematically in Figure 1. The model was constructed using four-node shell elements, where at each node, 6 DOF are considered; the varying shell thickness was modeled using the NREL specifications. This type of element was selected due to the type of problem at hand: the structure is, geometrically, a hollow tube constructed by a comparatively thin sheet of steel. The tower model was discretized into 2444 elements, with 2455 nodes, for a total 14,730 degrees of freedom. The elements can be assumed to be in plane strain, which allows performing a reduced order analysis. This assumption also impacts the cost of multiaxial fatigue computations, since the problem reduces to a biaxial problem. Nevertheless, the principles applied still hold for triaxial fatigue computations.

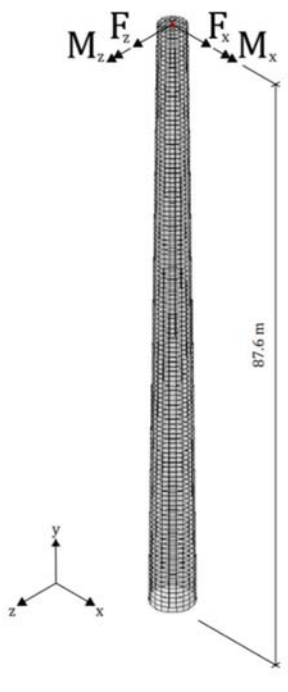

Figure 1. Equivalent system of forces at the RNA-tower interface.

The wind turbine simulation software FAST [22] was employed using the aforementioned tower model specifications. A simulation of 8 s was conducted, recreating operational wind conditions and loads on a tower model with the aforementioned specifications. The time history of the force transmitted through the RNA-tower interface was extracted. The obtained signal time history was subsequently used in the numerical analysis as the system input.

Structural matrices were obtained from the FE model shown in Figure 2, and a modal analysis was performed to obtain the corresponding natural frequencies and mode shape vectors. The dominating dynamic forces at the RNA interface pertaining to the wind loads and rotation dynamics were recorded as 2 concentrated loads and 2 concentrated moments, and frequency analysis was carried out on the input channels. Based on the frequency content of the input, we realized that the first 3 modes predominantly contribute to the system dynamical responses. The natural frequencies are reported in Table 1.

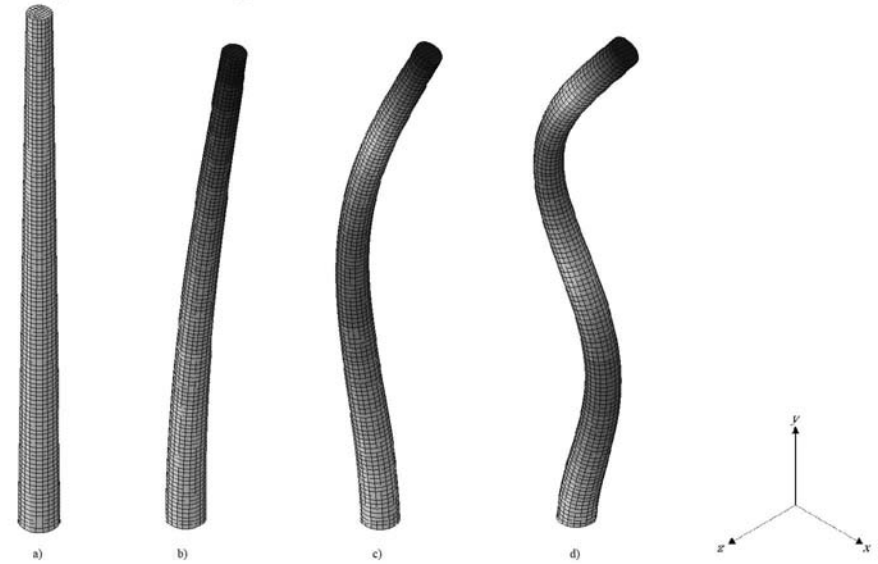

Figure 2: Finite element model of NREL's 5MW land-based wind turbine tower: a) base state, b) first mode, c) second mode, d) third mode.

Mode	Frequency (Hz)
1	0.8761
2	4.1737
3	10.395

Table 1: Finite element model natural frequencies.

The observation model was constructed from a limited number of output measurements; the discussion of stability of an Augmented Kalman Filter (AKF) presented by Lourens et al. [10] pointed out that ill-conditioning in the joint input-state estimator might increase depending on the sensor placement. Additionally, Maes et al. [23] suggested that the number of sensors should at least be equal to the number of forces to be identified. Thus, 2 biaxial acceleration and 4 strain responses were treated as the observed quantities. One set of collocated sensors, comprising 1 acceleration and 2 strain observations, was placed at a height of 86.9 m. from the ground, i.e. in the near-vicinity of the load application point; a similar second set of sensors was placed at a height of 63.5 m. from the ground. Figure 3 shows the locations of the response observations. Noise was introduced to the measurements as 1% of the root-mean-square deviation found in the observed channels, i.e. strains and accelerations.

A dynamic simulation of the first 8 s of operation was conducted. The structure is initially at rest, and the equivalent force system is applied at the beginning of the simulation. The modally-reduced state was estimated using the sequential Bayesian filter, and the full-field system response was reconstructed from the state and input estimation. The stress state time history at the finite element level is computed from a linear relationship between displacements and stresses under static loading cases. Consequently, accuracy in the estimation of nodal displacements is prescribed. Figures 4-5 show the acceleration and displacement, and stress responses, respectively, of an unmeasured near the base of the tower, i.e. a location far from the observations. The response estimates show agreement between the real and estimated responses. Notably, the estimated displacement responses were highly accurate. The stress and strain fields, however, do not display the same level of accuracy; thus, deviations from the real response in the displacement field are amplified in the corresponding stress field.

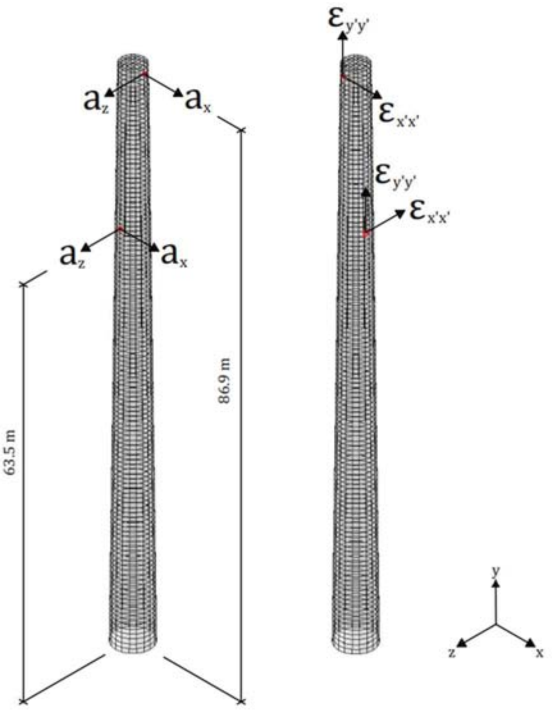

Figure 3: Measurement locations: a) accelerations, b) strains.

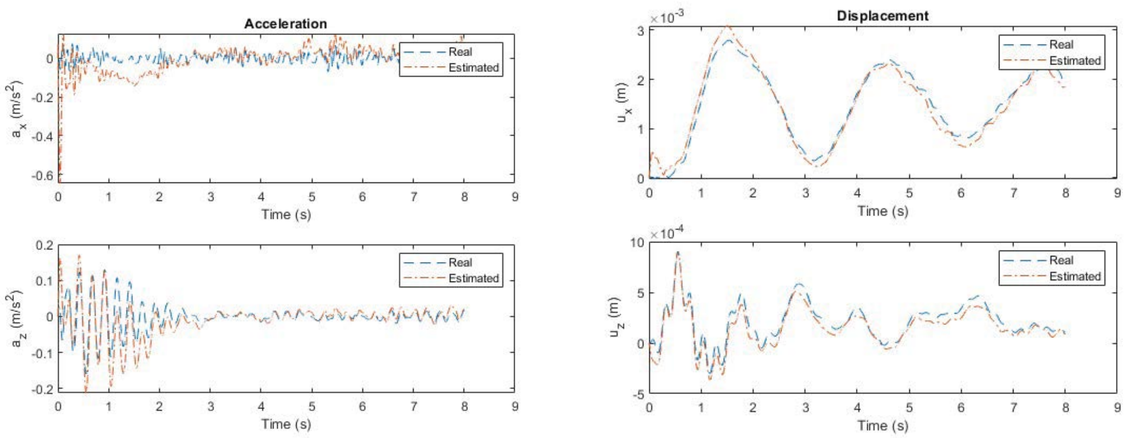

Figure 4: Real vs. estimated acceleration and displacement at unmeasured location near the tower base.

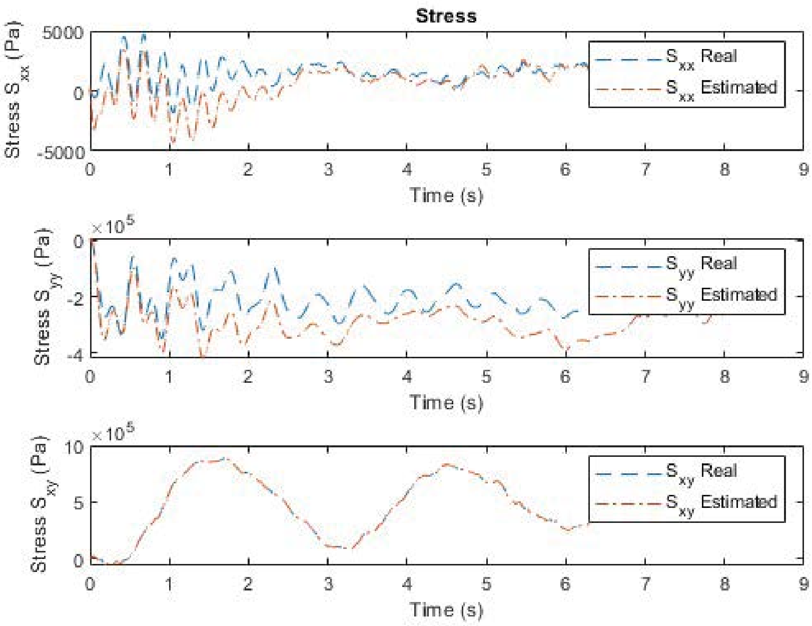

Figure 5: Real vs. estimated responses at unmeasured location near the tower base.

The next step is to identify the critical plane for each finite element by applying the MVM. Figure 6 shows the real and estimated shear stresses resolved along the critical plane. Considering that the shear stress transformation is a function of the stress state, it is evident that the error in the critical plane shear stress depends greatly on the accuracy of the stress tensor estimate. The normal stresses σ_{xx} and σ_{yy} are markedly influenced by the drift in the response estimations. The critical plane shear stress time histories are used to compute the stress amplitude range and the number of cycles at each amplitude range by means of the RCM.

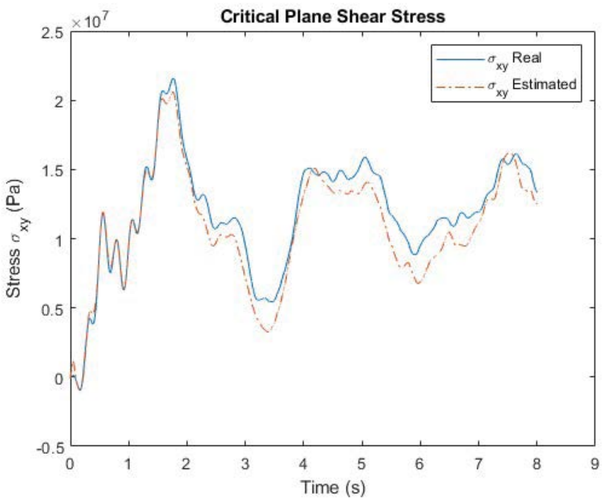

Figure 6: Shear stress resolved along the critical plane.

Lastly, a Modified Wöhler Curve and the linear Palmgren-Miner's rule are applied to compute the accumulated fatigue damage at each finite element. A full-field damage accumulation map and the resulting error are shown in Figures 7-8. The error in the fatigue damage estimation is caused by the deviations in the critical plane shear stress: the error is carried over to the cycle counting, and thence to the damage accumulation computation.

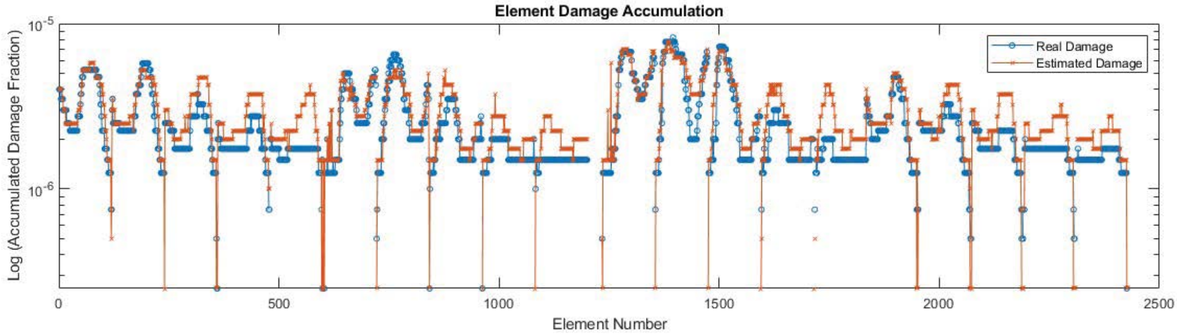

Figure 7: Full-field fatigue damage accumulation.

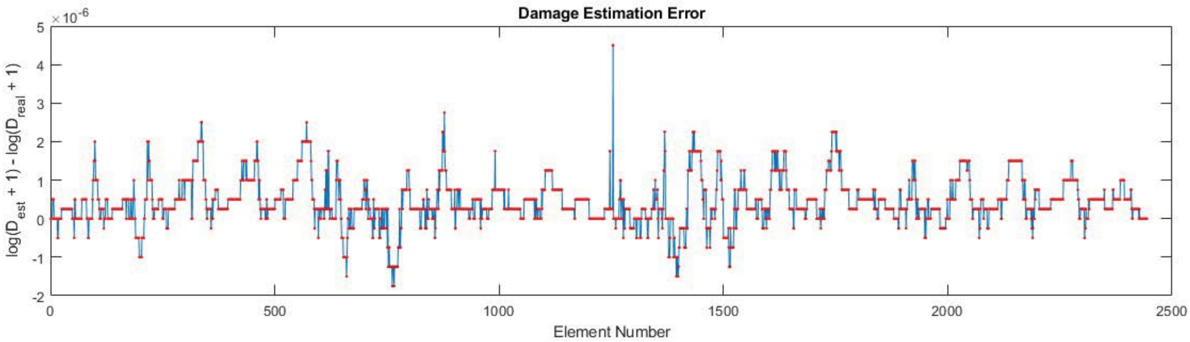

Figure 8: Damage estimation error.

6 CONCLUSION

A framework for computing full-field fatigue damage accumulation from a limited number of output-only measurements was presented. The proposed methodology promises real-world applicability on a variety of structures under unknown excitations, provided the proper calibration of the estimation algorithm is exercised, and an optimal observation location configuration is implemented. Its capability to efficiently produce a full-field fatigue map from limited measurements makes it a powerful tool for monitoring fatigue accumulation in wind turbine tower structures.

7 ACKNOWLEDGEMENTS

Financial support from the Hong Kong Research Grants Council under project No. 16234816, 16212918, and 16211019 is gratefully acknowledged. The first author would like to express his gratitude to the Mexican National Council for Science and Technology CONACYT for its support.

REFERENCES

[1] C. Papadimitriou, C.-P. Fritzen, P. Kraemer, and E. Ntotsios, “Fatigue predictions in entire body of metallic structures from a limited number of vibration sensors using Kalman filtering,” *Struct. Control Heal. Monit.*, vol. 18, no. 5, pp. 554–573, Aug. 2011.

[2] C. Papadimitriou, E. Lourens, G. Lombaert, G. De Roeck, and K. Liu, “Prediction of fatigue damage accumulation in metallic structures by the estimation of strains from

operational vibrations," in *Life-Cycle and Sustainability of Civil Infrastructure Systems: Proceedings of the Third International Symposium on Life-Cycle Civil Engineering (IALCCE'12), Vienna, Austria, October 3-6, 2012*, 2012, p. 103.

[3] K. Tatsis, V. Dertimanis, I. Abdallah, and E. Chatzi, "A substructure approach for fatigue assessment on wind turbine support structures using output-only measurements," *Procedia Eng.*, vol. 199, pp. 1044–1049, Jan. 2017.

[4] N. Noppe, K. Tatsis, E. Chatzi, C. Devrient, and W. Weijtjens, "Fatigue stress estimation of offshore wind turbine using a Kalman filter in combination with accelerometers," in *Proceedings of International Conference on Noise and Vibration Engineering (ISMA 2018), International Conference on Uncertainty in Structural Dynamics (USD 2018)*, 2018, pp. 4693–6701.

[5] K. Maes, A. Iliopoulos, W. Weijtjens, C. Devriendt, and G. Lombaert, "Dynamic strain estimation for fatigue assessment of an offshore monopile wind turbine using filtering and modal expansion algorithms," *Mech. Syst. Signal Process.*, vol. 76–77, pp. 592–611, Aug. 2016.

[6] S. P. Tchemodanova, K. Tatsis, V. Dertimanis, E. Chatzi, and M. Sanayei, "Remaining Fatigue Life Prediction of a Roller Coaster Subjected to Multiaxial Nonproportional Loading Using Limited Measured Strain Locations," in *Structures Congress 2019: Bridges, Nonbuilding and Special Structures, and Nonstructural Components*, 2019, pp. 112–121.

[7] S. Eftekhar Azam, E. Chatzi, and C. Papadimitriou, "A dual Kalman filter approach for state estimation via output-only acceleration measurements," *Mech. Syst. Signal Process.*, vol. 60–61, pp. 866–886, Aug. 2015.

[8] D.-C. Papadioti, "Management of uncertainties in structural response and reliability simulations using measured data," University of Thessaly (UTH), 2015.

[9] E. Lourens, C. Papadimitriou, S. Gillijns, E. Reynders, G. De Roeck, and G. Lombaert, "Joint input-response estimation for structural systems based on reduced-order models and vibration data from a limited number of sensors," *Mech. Syst. Signal Process.*, vol. 29, pp. 310–327, May 2012.

[10] E. Lourens, E. Reynders, G. De Roeck, G. Degrande, and G. Lombaert, "An augmented Kalman filter for force identification in structural dynamics," *Mech. Syst. Signal Process.*, vol. 27, no. 1, pp. 446–460, Feb. 2012.

[11] D. Teymouri, O. Sedehi, L. S. Katafygiotis, and C. Papadimitriou, "A new online Bayesian approach for the joint estimation of state and input forces using response-only measurements," in *13th International Conference on Applications of Statistics and Probability in Civil Engineering, ICASP 2019*, 2019.

[12] V. K. Dertimanis, E. N. Chatzi, S. Eftekhar Azam, and C. Papadimitriou, "Input-state-parameter estimation of structural systems from limited output information," *Mech. Syst. Signal Process.*, vol. 126, pp. 711–746, Jul. 2019.

[13] O. Sedehi, C. Papadimitriou, D. Teymouri, and L. S. Katafygiotis, "Sequential Bayesian estimation of state and input in dynamical systems using output-only measurements," *Mech. Syst. Signal Process.*, vol. 131, pp. 659–688, Sep. 2019.

[14] U. Lagerblad, H. Wentzel, and A. Kulachenko, "Dynamic response identification based on state estimation and operational modal analysis," *Mech. Syst. Signal Process.*, vol. 129, pp. 37–53, Aug. 2019.

[15] D. Socie and G. Marquis, *Multiaxial fatigue*. Warrendale, Pa.: Society of Automotive Engineers, 2000.

[16] L. Susmel, "A simple and efficient numerical algorithm to determine the orientation of the critical plane in multiaxial fatigue problems," *Int. J. Fatigue*, vol. 32, no. 11, pp.

1875–1883, Nov. 2010.
[17] L. Susmel and R. Tovo, "Estimating fatigue damage under variable amplitude multiaxial fatigue loading," *Fatigue Fract. Eng. Mater. Struct.*, vol. 34, no. 12, pp. 1053–1077, Dec. 2011.
[18] L. Susmel and P. Lazzarin, "A bi-parametric Wohler curve for high cycle multiaxial fatigue assessment," *Fatigue Fract. Eng. Mater. Struct.*, vol. 25, no. 1, pp. 63–78, Jan. 2002.
[19] A. Palmgren, "Die lebensdauer von kugellargern," *Zeitshrift des Vereines Duetsher Ingenieure*, vol. 68, no. 4, p. 339, 1924.
[20] M. A. Miner, "Cumulative fatigue damage," *J. Appl. Mech.*, vol. 12, no. 3, pp. A159–A164, 1945.
[21] J. Jonkman, S. Butterfield, W. Musial, and G. Scott, "Definition of a 5-MW reference wind turbine for offshore system development," Golden, CO, 2009.
[22] J. Jonkman and B. Jonkman, "NWTC Information Portal (FAST)," 2018. [Online]. Available: https://nwtc.nrel.gov/FAST.
[23] K. Maes, E. Lourens, K. Van Nimmen, E. Reynders, G. De Roeck, and G. Lombaert, "Design of sensor networks for instantaneous inversion of modally reduced order models in structural dynamics," *Mech. Syst. Signal Process.*, vol. 52–53, no. 1, pp. 628–644, 2015.